Upper Triassic to Lower Jurassic stratigraphy of the Faro Peak formation, southern Tay River map area, central Yukon (NTS 105K)

A.C. Wiest, L.P. Beranek* and M.J. Manor
Department of Earth Sciences, Memorial University of Newfoundland

Wiest, A.C., Beranek, L.P. and Manor, M.J., 2020. Upper Triassic to Lower Jurassic stratigraphy of the Faro Peak formation, southern Tay River map area, central Yukon (NTS 105K). *In:* Yukon Exploration and Geology 2019, K.E. MacFarlane (ed.), Yukon Geological Survey, p. 121–139.

Abstract

The lower and upper members of the Faro Peak formation comprise Upper Triassic and Lower Jurassic successions, respectively, that are assigned to the Yukon-Tanana terrane in the southern Tay River map area (NTS 105K). The lower member is ~650 m-thick and contains a basal conglomerate overlain by argillite, limestone, basalt, and lithic feldspathic wacke to arenite that represents part of an overlap assemblage and regionally covers Paleozoic rocks of the Yukon-Tanana terrane, Slide Mountain terrane, and ancestral Cordilleran margin. The upper member has >800 m of massive conglomerate and sandstone that overlies different stratigraphic levels of the lower member and locally sits on Yukon-Tanana basement. The upper member is coeval with Whitehorse trough strata of central Yukon and similarly records Early Jurassic exhumation of the northern Intermontane terranes. The two members are lithologically distinct, of mappable extent, and have unconformable contacts, and therefore should be separated into two new formations.

* lberanek@mun.ca

Introduction

The late Permian to Early Jurassic was a time of significant change along the northwestern margin of North America. The deposition of multiple syn to post-orogenic sedimentary successions from eastern Alaska to northern British Columbia (Fig. 1; Mihalynuk et *al*., 1994; Beranek and Mortensen, 2011; Colpron et *al*., 2015; Golding et *al*., 2016) was related to arc accretion, outward stepping of the continental margin, new arc development, and crustal thickening and exhumation of the Intermontane terranes (*e.g.*, Yukon-Tanana, Slide Mountain, Stikinia, Quesnellia, Cache Creek). Middle to Upper Triassic overlap assemblages were deposited across the Yukon-Tanana and Slide Mountain terranes and former Cordilleran margin after late Permian closure of a marginal ocean basin (Beranek and Mortensen, 2011). Yukon-Tanana terrane basement rocks were locally metamorphosed to eclogite facies during this ocean closure and contain late Permian white mica cooling ages in the Faro area of central Yukon (Erdmer et *al*., 1998). Subsequent Late Triassic to Early Jurassic arc collision and intra-arc shortening along the composite margin resulted in regional crustal thickening and burial of Stikinia and Yukon-Tanana basement to mid-crustal depths (Johnston et *al*. 1996; Topham et *al*., 2016; Clark, 2017). This crustal thickening in central Yukon was followed by ~15-20 km of tectonic exhumation (Knight et *al*., 2013) and resulted in Sinemurian and later deposition of Laberge Group strata in the Whitehorse trough (Fig. 1; Colpron et *al*., 2015; Staples et *al*., 2016). Dusel-Bacon et *al*. (2002) similarly documented Early Jurassic exhumation in the Yukon-Tanana terrane of eastern Alaska after regional crustal thickening. Constraining the timing and depositional setting of Late Triassic to Early Jurassic basin-filling events is critical to investigate these existing models and further constrain the tectonic evolution and growth of the Canadian Cordillera.

Isolated exposures of Upper Triassic to Lower Jurassic rocks assigned to the Faro Peak formation by Pigage (2004) crop out along the Yukon-Tanana–Slide Mountain terrane boundary near the town of Faro (Fig. 2a,b) in the southern Tay River map area (NTS 105K). Colpron et *al*. (2015) reported 200–180 Ma detrital zircon grains in conglomerate units of the Faro Peak formation and correlated these rock units with synorogenic strata of the Laberge Group in central Yukon and northern British Columbia. A two-year project was initiated in 2018 to test these hypotheses (Wiest and Beranek, 2019) and investigate the depositional age, regional correlation, and tectonic setting of the Faro Peak formation.

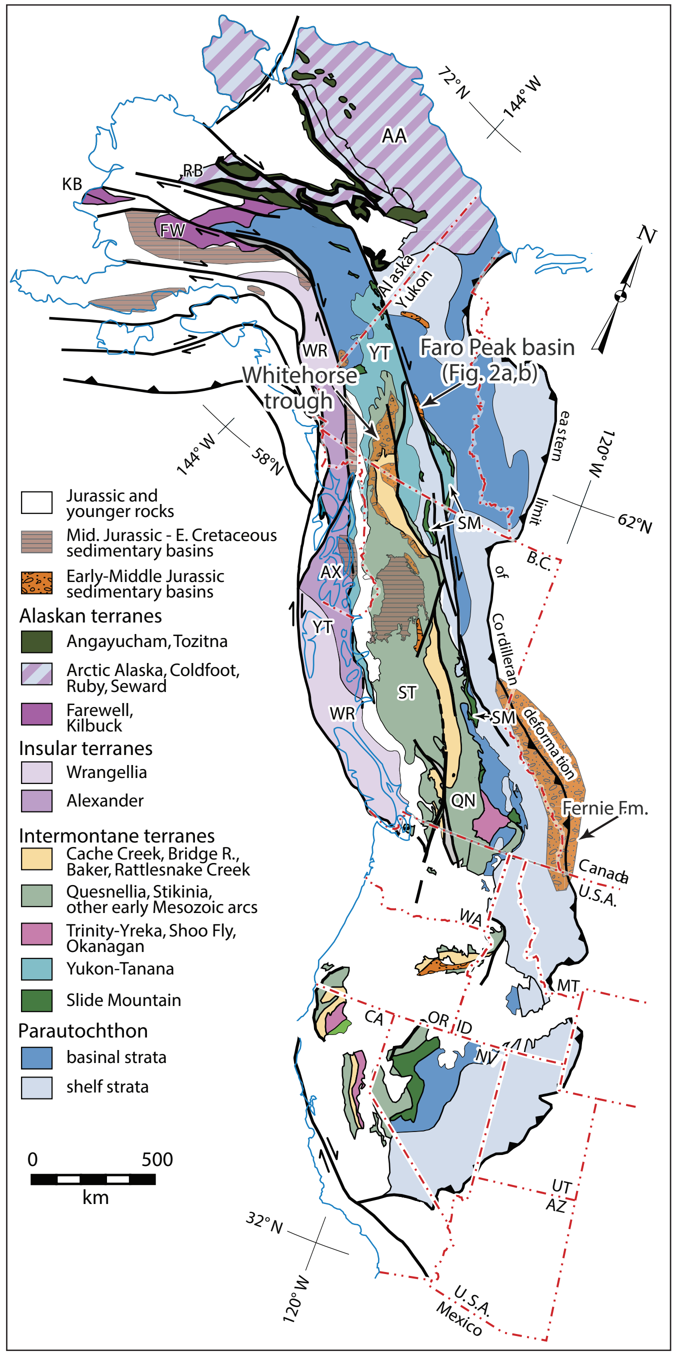

Figure 1. *Paleozoic to early Mesozoic terrane map of the North American Cordillera and associated Jurassic basins modified from Colpron et al. (2015). Terrane abbreviations: AA–Arctic Alaska; AX–Alexander; FW–Farewell; KB–Kilbuck; QN–Quesnellia; RB–Ruby; SM–Slide Mountain; ST–Stikinia; YT–Yukon-Tanana.*

In this article, we summarize our 2019 field studies and current understanding of the Faro Peak formation as originally defined by Pigage (2004). The internal character of the lower member of the Faro Peak formation is documented in a new stratigraphic section west of Rose Mountain. The contact between the upper and lower members of the Faro Peak formation appears to be transitional in at least two localities. The observation that upper member conglomerate overlies multiple units of the lower member and quartzite and schist units of the Yukon-Tanana terrane suggests, however, that the base of the upper member is an unconformity. Finally, we speculate on the basis of lithological differences and unconformable contacts that some or all rocks previously included in the lower Faro Peak formation should be re-assigned to a new formation. It is currently uncertain if all lower member units of Pigage (2004) should be included in this new formation. Ongoing detrital zircon U-Pb-Hf isotope and petrographic investigations of Faro Peak formation rock units will assist in future stratigraphic correlations and help guide a new formation designation.

Geological background

The town of Faro is located at the eastern edge of the Intermontane belt near the suture between the Yukon-Tanana and Slide Mountain terranes (Fig. 2a,b). In this area, the Intermontane terranes are separated from parautochthonous North American continental margin strata along the Inconnu thrust to the northeast and Cassiar terrane along the Tintina fault to the southwest (Fig. 2a,b; Pigage, 2004). Dextral movement along the Tintina fault accommodated at least 430 km of

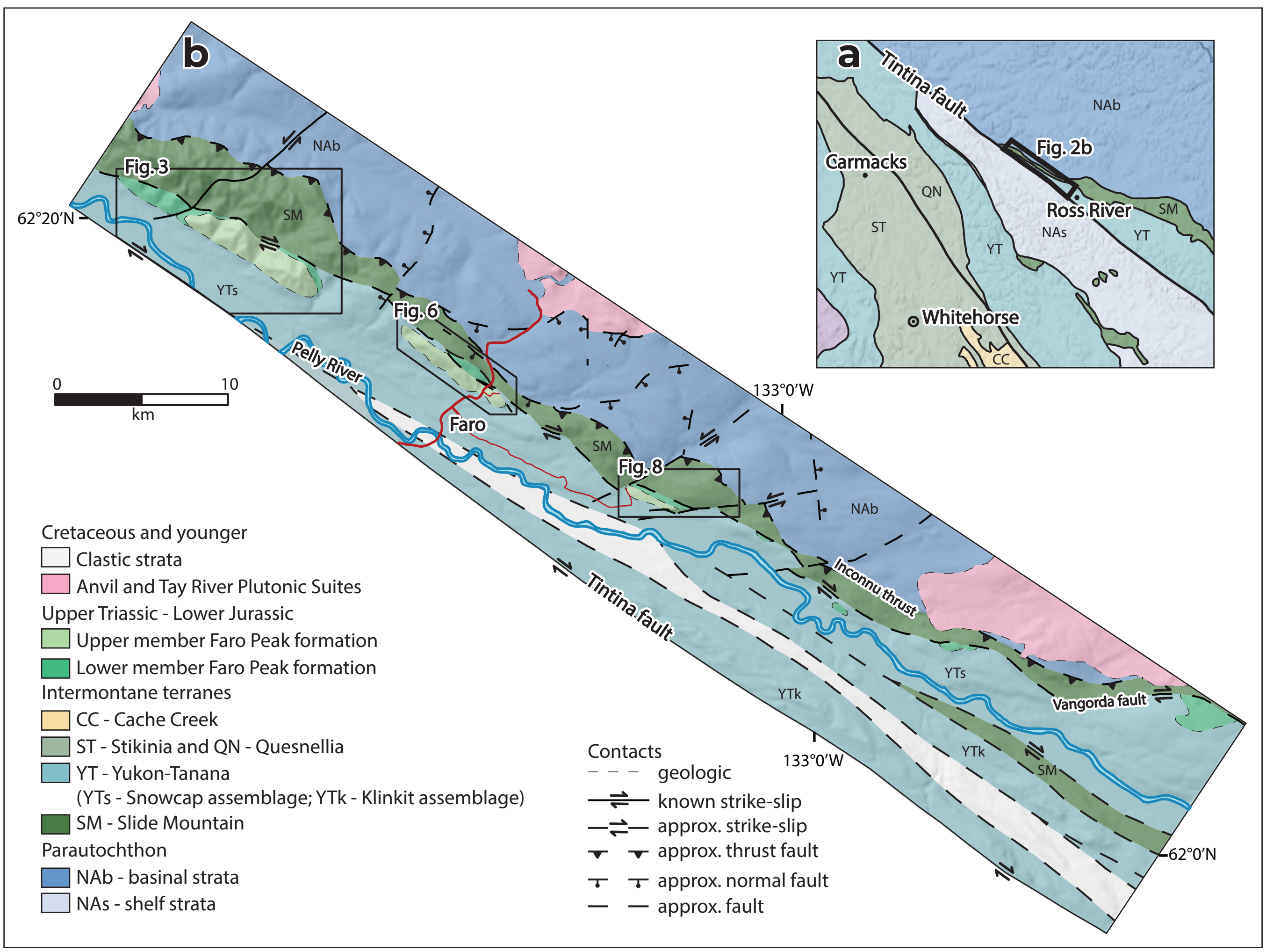

Figure 2. (a) *Terrane map of central Yukon modified from Yukon Geological Survey (2019).* **(b)** *Simplified bedrock geology of the southern Tay River map area modified from Pigage (2004).*

post-Cretaceous displacement (Gabrielse et *al.*, 2006). Restoration of the Tintina fault places Faro near the present day region of Eagle, Alaska. In the Faro area, the Yukon-Tanana and Slide Mountain terranes are separated by the Vangorda fault (Fig. 2b), a northern equivalent to the Jules Creek fault in the Finlayson Lake map area (Murphy et *al.*, 2006).

The Faro Peak formation crops out along a northwest-trending belt that parallels the Tintina Trench near Faro. Faro Peak formation strata were first described by Tempelman-Kluit (1972, 1979) as argillaceous limestone, silty slate, and polymictic conglomerate that unconformably overlies quartzite, schist, and other metasedimentary rocks of what is now called the Snowcap assemblage (*e.g.* Colpron et *al.*, 2006) of the Yukon-Tanana terrane. Pigage (2004) informally named the Faro Peak formation and defined a lower member of basal basalt overlain by interbedded argillite, chert, greywacke, limestone, and conglomerate, and an upper member of massive, polymictic conglomerate. Wiest and Beranek (2019) documented that these lower and upper member units were deposited in contrasting environments. Lower member units ~3 km northeast of the Faro township exhibit normally graded, tabular, and convolute bedding characteristics that are generally consistent with deposition by turbulent, concentrated density flows. Petrographic results indicate that some lower member sandstone units have mafic to intermediate volcanic provenance (Wiest and Beranek, 2019). Massive, upper member conglomerate and channelized sandstone units from Faro Peak and adjacent ridges are consistent with deposition by non-concentrated debris flows. Typical clasts in the upper member conglomerate units include schist, quartzite, chert, and mafic to felsic intrusive rocks, which suggests that the upper Faro Peak formation has provenance from Intermontane terrane basement assemblages and may be linked to depositional events along the Vangorda fault or its predecessor (*c.f.* Tempelman-Kluit, 1972).

2019 field observations

Lower member of the Faro Peak formation

Rose Mountain

The lower member of the Faro Peak formation near Rose Mountain, ~20 km northwest of Faro, is ~650 m-thick and generally undeformed (Figs. 3 and 4). Lower member units at this location unconformably overlie micaceous quartzite and schist of the Snowcap assemblage (Fig. 5a). The basal unconformity is defined by well-silicified, pebble to cobble conglomerate that contains clasts of schist, quartzite, black to grey chert, and tan volcanic rocks (Fig. 5b). This basal conglomerate is overlain by interbedded graphitic to calcareous shale and tan weathering, dark grey micrite (Fig. 5c). Limestone from this succession yields Late Triassic conodont elements (Late Norian to Rhaetian *M. ex gr. Polygnathiformis*, Late Carnian *Epigondolella cf. mosheri* and *Norigondolella steinbergensis*; Pigage, 2004; Orchard, 2006). Conformably above this limestone is an ~4 m-thick exposure of grey basalt and green lithic feldspathic wacke units that become sheared upsection (Fig. 5d,e). Shearing at this locality is interpreted to be intraformational bedding plane movement that occurred along the resistant basalt-wacke contact (cf., Tempelman-Kluit, 1979). Poorly exposed argillaceous to silty micrite beds that show cross-stratification overlie this sheared section (Fig. 5f). Along strike ~1 to 2 km to the southeast, limestone units are mapped as being interbedded with basalt and wacke units (Jennings et *al.*, 1978; Pigage, 2004). Exposures above the cross-stratified limestone units are rare. Small outcrop of thinly laminated, dark grey micrite and micaceous siltstone were observed directly against the Vangorda fault, which separates the lower member from foliated serpentinite and gabbro of the Slide Mountain terrane (Fig. 3).

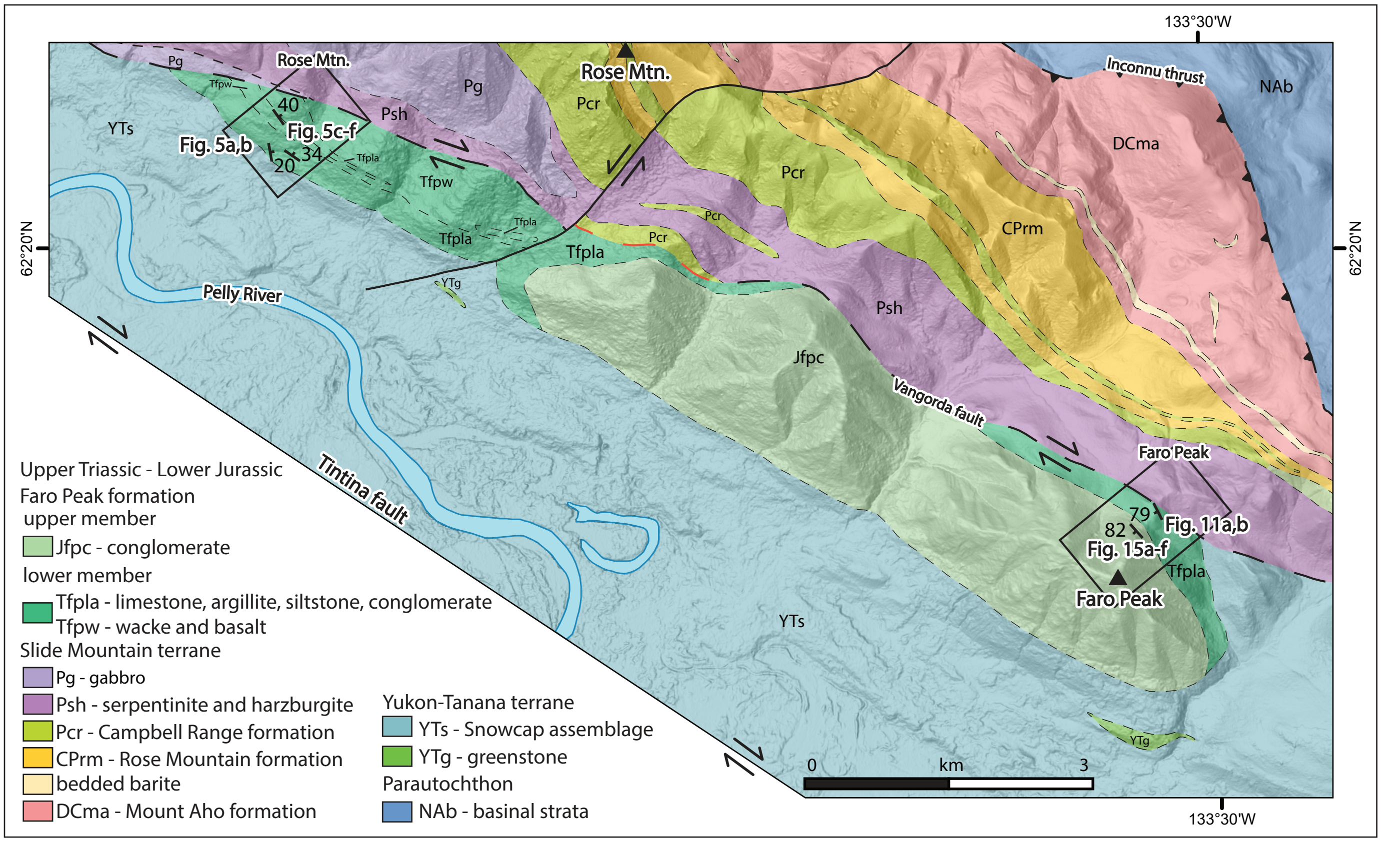

Figure 3. *Simplified bedrock geology map of the Rose Mountain and Faro Peak areas discussed in the text (modified from Pigage, 2004 and Jennings et al., 1978). Red dashed line indicates modified Vangorda fault location due to reassignment of basalt unit to Campbell Range formation. Contact symbols same as Figure 2. Basemap DEM (digital elevation model) obtained from the University of Minnesota Polar Geospatial Center (2018) and Porter et al. (2018).*

Repeater Hill

Late Triassic conodont elements (late Norian; *Epigondolella quadrata*; Orchard, 2006) are reported in dark grey micrite to wackestone units below the NorthwesTel repeater at the top of Repeater Hill, ~22 km to the southeast of Rose Mountain and ~2.5 km northwest of Faro (Fig. 6). Upper Triassic limestone units are interbedded with siltstone and argillite units similar to those at Rose Mountain, however, at Repeater Hill these fine-grained strata are strongly foliated along a fault that cuts out the basal conglomerate and juxtaposes younger lower member rocks with the Snowcap assemblage (Fig. 7a,b).

Blind Creek–Dena Cho Trail

The Blind Creek–Dena Cho Trail localities are ~10 km southeast of the Faro townsite (Fig. 8). Near the trace of the Vangorda fault, mineral exploration trenches provide access to lower member outcrops in otherwise unexposed areas. The lower member typically consists of foliated, thin-bedded, dark grey micrite, siltstone, and argillite units (Fig. 9a,b). There are no reported fossil constraints on the limestone units in this area.

Eastern Whiskey Mountain

Lower member strata exposed along the eastern ridge of Whiskey Mountain, ~3 km northeast of Faro (Fig. 6), are generally more coarse-grained than the argillite and limestone-dominated units at the Rose Mountain and Repeater Hill localities. Stratigraphic relationships along the eastern ridge of Whiskey Mountain are uncertain because of poor exposure and variable bedding. Rock units along the north fork of Vangorda Creek appear highly deformed and contain east-verging folds and small-scale west-dipping faults (Fig. 10a,b).

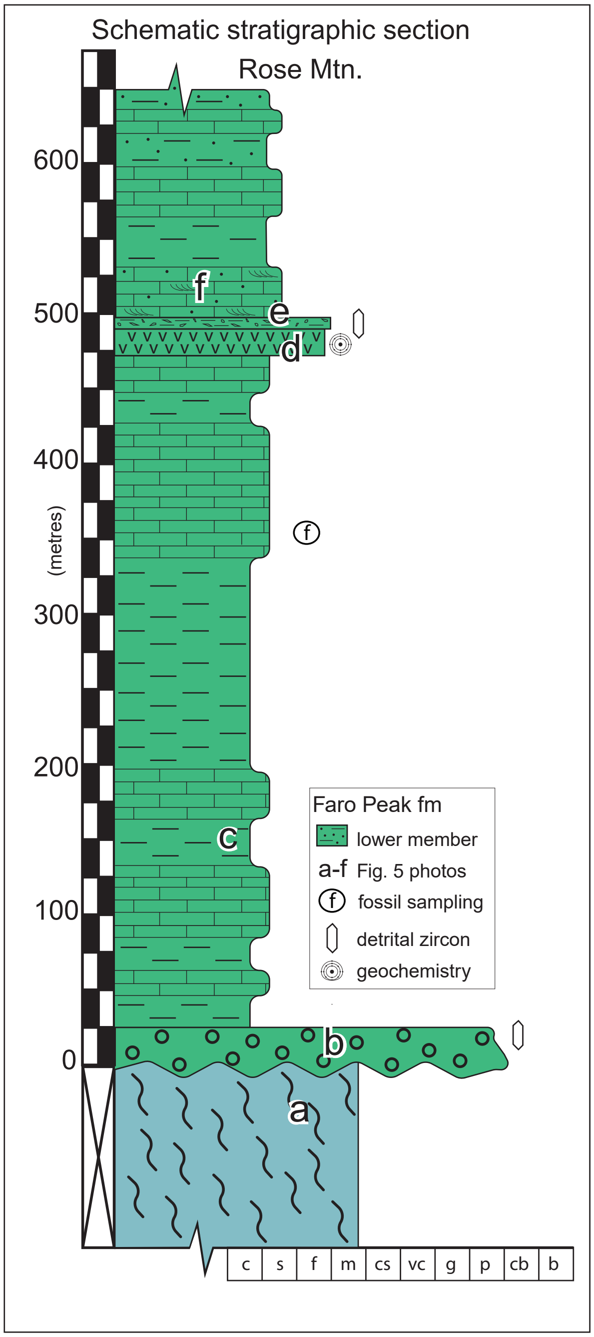

Figure 4. *Schematic stratigraphic section of the lower member of the Faro Peak formation at Rose Mountain. The fossil location is approximate. Samples are from the 2019 field season. Abbreviations: c–clay; s–silt; f–fine sand; m–medium sand; cs–coarse sand; vc–very coarse sand; g–gravel; p–pebble; cb–cobble; b–boulder.*

Green to grey volcanic lithic feldspathic wacke and feldspathic arenite units characterize this locality. Along the north fork of Vangorda Creek, thin to medium beds of orange to tan, fine to medium-grained, feldspathic arenite are interbedded with siltstone and argillite (Fig. 10c). Slightly coarser sandstone layers show evidence of slump structures or convolute bedding (Fig. 10d). Argillite is green to grey, thin bedded to massive, and locally contains minor white mica (Fig. 10e). A unit of green lithic feldspathic wacke reported by Wiest and Beranek (2019) is interpreted to be a sheet sand above isoclinally folded beds that are the result of soft sediment deformation. This same sheet sand was observed during this field season to overlie tabular to slightly undulatory, thin-bedded argillite and siltstone indicating that soft sediment deformation was local (Fig. 10f). The highest elevation exposures along the eastern ridge of Whiskey Mountain consist of tabular, medium to thick-bedded sheets of steeply dipping, medium to very coarse grained, feldspathic to lithic feldspathic arenite and siltstone interbeds (Fig. 10g,h).

Faro Peak

Northeast of Faro Peak, ~10 km northeast of Faro, the Vangorda fault separates serpentinite and harzburgite units of the Slide Mountain terrane from the lower member Faro Peak formation (Fig. 3). Lower member units at this locality consist of subvertical, grey to brown, thin-bedded, locally wavy laminated, micaceous argillite, siltstone, and feldspathic arenite units (Fig. 11a). These siliciclastic rock units grade upwards into resistant, tabular siltstone (Fig. 11b).

Interpretation

The lower member consists of three lithological groups: (1) interbedded shale/argillite and limestone units from Rose Mountain, Repeater Hill, and Blind Creek–Dena Cho Trail; (2) basalt, wacke, and lithic feldspathic arenite units from Rose Mountain and eastern Whiskey Mountain; and (3) micaceous siltstone, argillite, and feldspathic to lithic feldspathic arenite units from Faro Peak.

Figure 5. *Field photographs of the Snowcap assemblage (Sa) and lower member of the Faro Peak formation (FPf) at Rose Mountain.* ***(a)*** *Highly deformed micaceous schist and quartzite (Sa);* ***(b)*** *cut section of basal conglomerate unit (FPf);* ***(c)*** *interbedded shale and limestone (FPf);* ***(d)*** *grey basalt overlain by green wacke (FPf);* ***(e)*** *sheared green wacke; and* ***(f)*** *cross-stratified silty limestone. Yellow-handled hammer (55 cm) and brown-handled hammer (33 cm) for scale.*

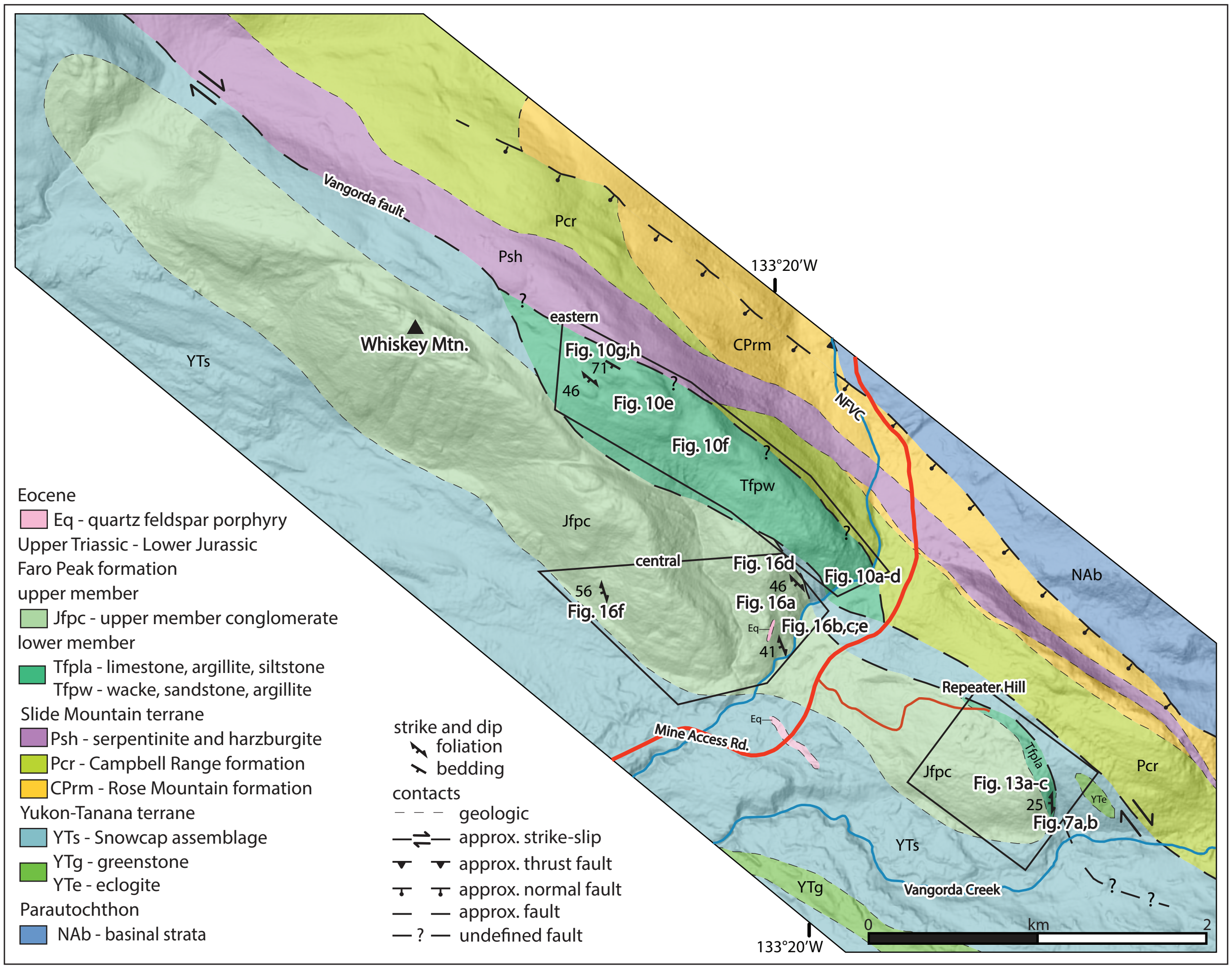

Figure 6. Simplified bedrock geology of the eastern and central Whiskey Mountain and Repeater Hill areas (modified from Pigage, 2004). Abbreviations: NFVC–north fork Vangorda Creek. Basemap DEM (digital elevation model) obtained from the University of Minnesota Polar Geospatial Center (2018) and Porter et al. (2018).

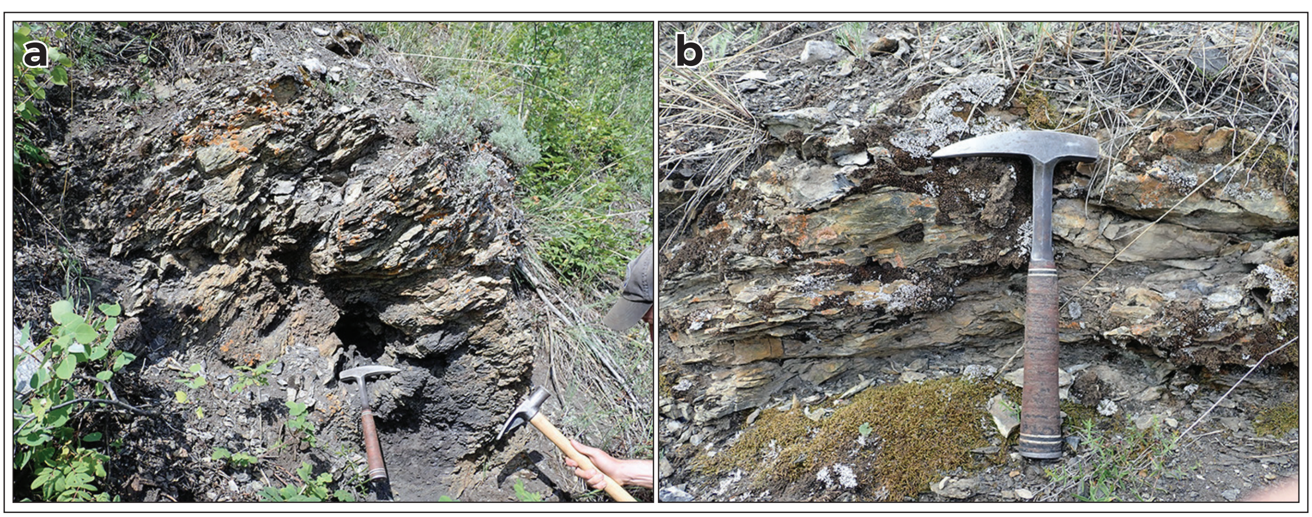

***Figure 7.** Field photographs of the lower member of the Faro Peak formation at Repeater Hill. **(a)** Strongly foliated argillite and siltstone; and **(b)** thin-bedded, tan weathered, dark grey micrite. Yellow-handled hammer (55 cm) and brown-handled hammer (33 cm) for scale.*

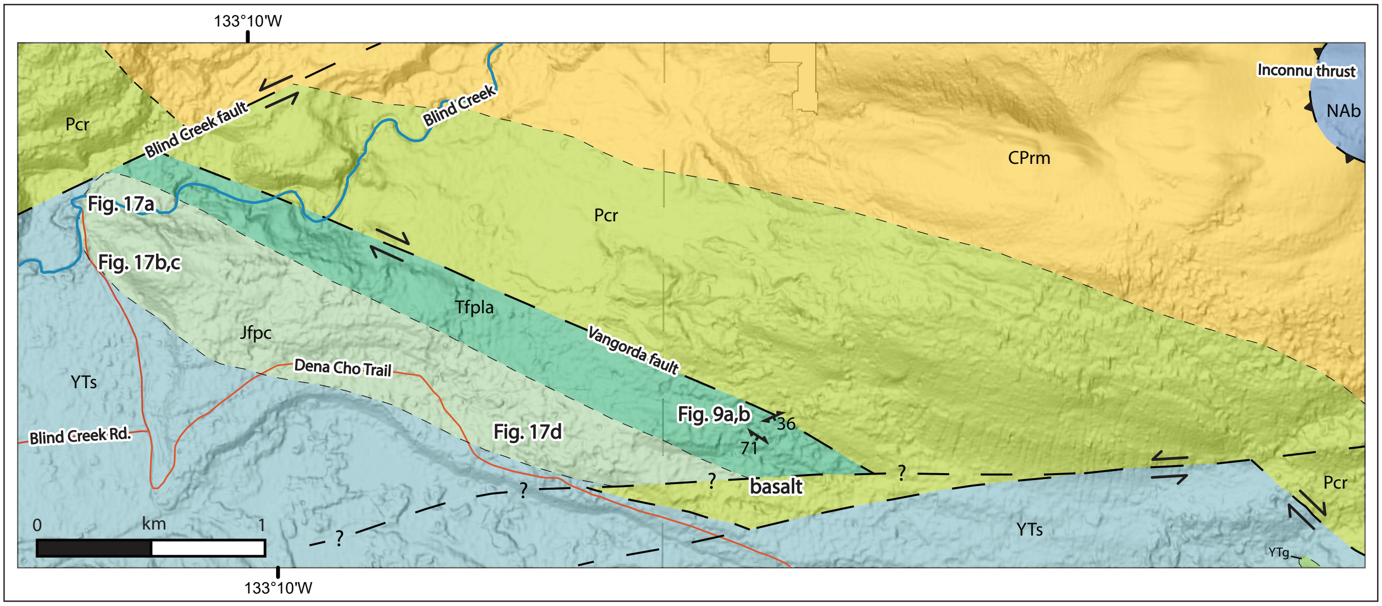

Figure 8. *Simplified bedrock geology of the Blind Creek and Dena Cho Trail area (modified from Pigage, 2004). Symbols same as Figure 6. Basemap DEM obtained from the University of Minnesota Polar Geospatial Center (2018) and Porter et al. (2018).*

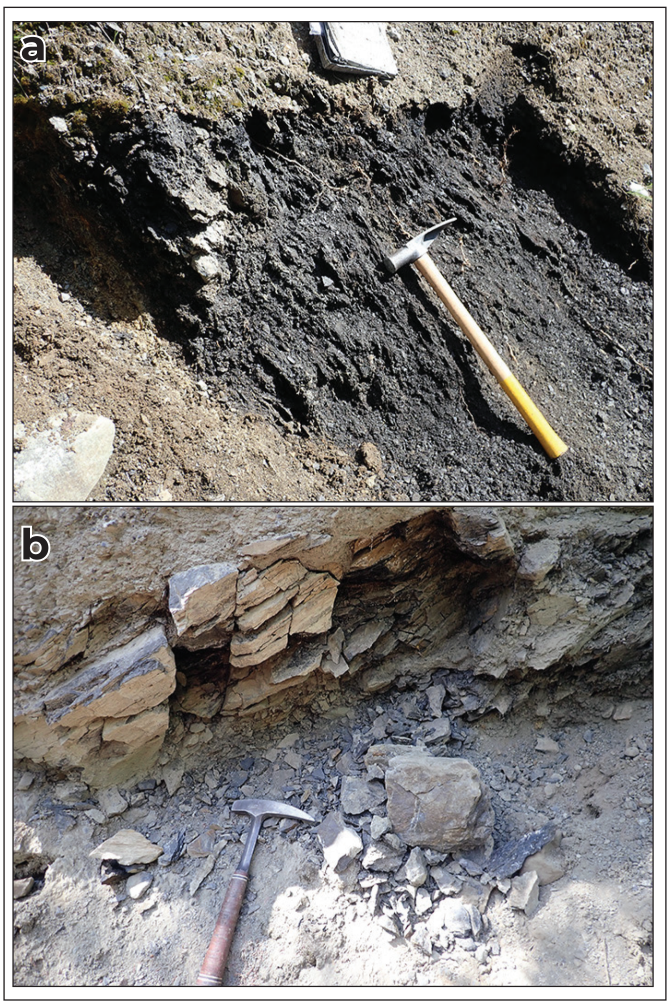

Figure 9. *Field photographs of the lower member of the Faro Peak formation near the Dena Cho Trail and Vangorda fault.* ***(a)*** *Trenched outcrop of foliated argillite; and* ***(b)*** *trenched outcrop of tan weathered, dark grey micrite.*

Upper Triassic limestone and shale units are age-constrained by conodont fossils in the lower part of the Rose Mountain section and sit unconformably on metasedimentary rocks of the Snowcap assemblage. These basal units are interpreted to correlate with Upper Triassic argillite and fossil-bearing limestone units that crop out at the Repeater Hill locality. The overlying basalt-wacke succession at Rose Mountain is likely correlative with green wacke and arenite units along the eastern ridge of Whiskey Mountain (Fig. 12), suggesting that the latter comprise the upper portion of the lower member. The basalt-wacke succession at Rose Mountain apparently indicates a shift from earlier, argillite-limestone deposition to proximal derivation from mafic to intermediate volcanic rocks. For example, Wiest and Beranek (2019) reported that lithic feldspathic arenite units along the eastern ridge of Whiskey Mountain contain angular mafic to intermediate volcanic rock fragments and suggest local, first-cycle sources. The uppermost parts of the lower member at Rose Mountain include micrite and micaceous siltstone that potentially correlate with micaceous argillite,

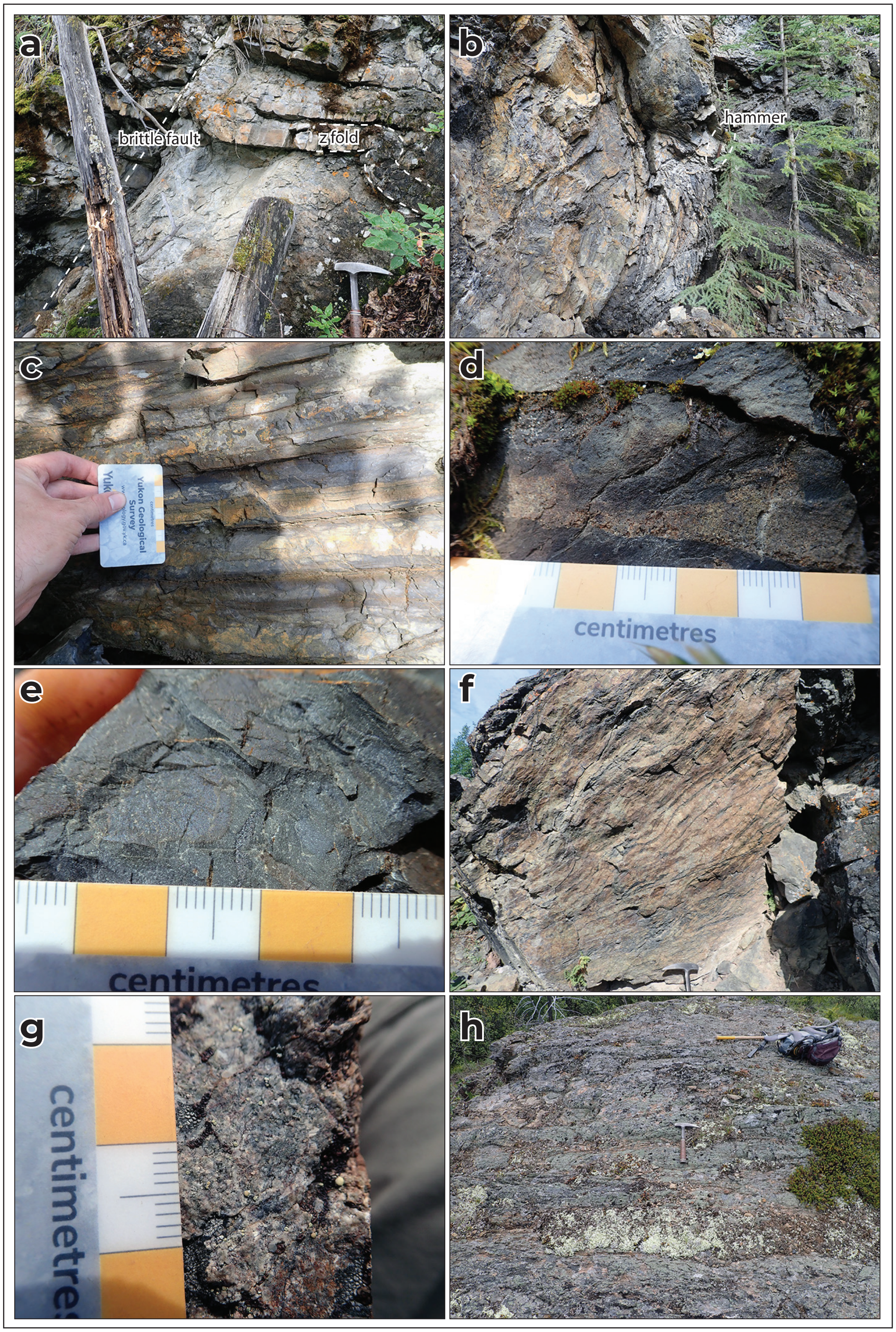

Figure 10. *Field photographs of the lower member of the Faro Peak formation at eastern Whiskey Mountain.* **(a)** *West-dipping brittle fault in argillite and medium-grained tabular sandstone with z-fold;* **(b)** *west-dipping brittle fracture in thin-bedded siltstone and fine-sandstone with east-vergent box-fold;* **(c)** *tabular bedded siltstone and argillite with local scouring* **(d)** *slump structure in coarse sandstone and argillite;* **(e)** *massive green argillite;* **(f)** *tabular, undulatory-bedded argillite and siltstone;* **(g)** *immature coarse-grained feldspathic arenite; and* **(h)** *steeply-dipping, tabular-bedded sandstone and siltstone. Brown-handled hammer (33 cm) for scale.*

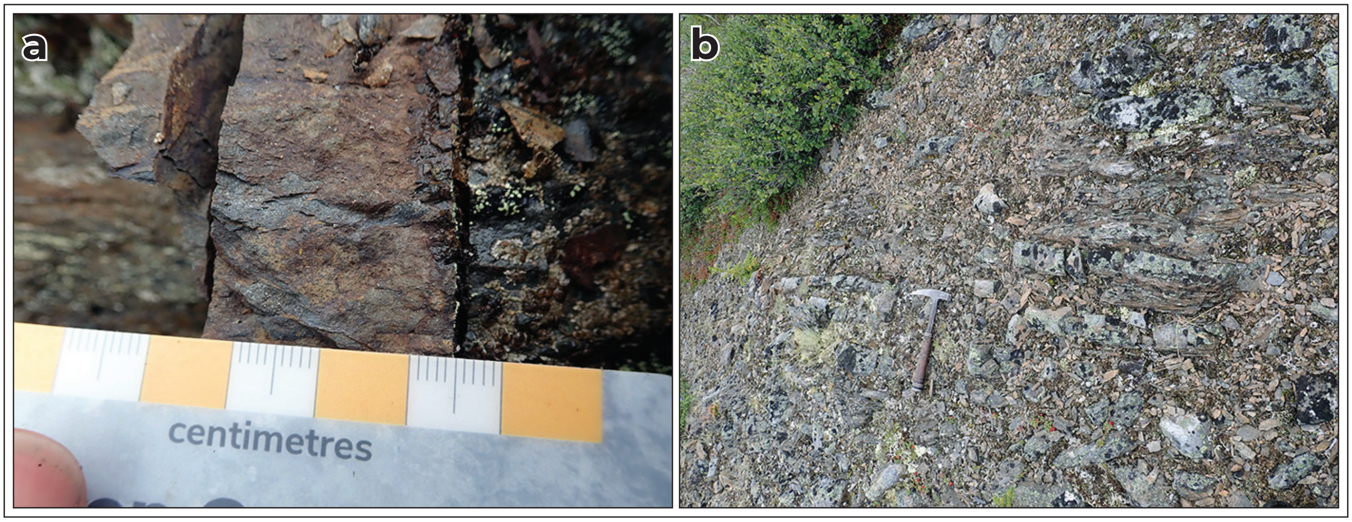

Figure 11. *Field photographs of the lower member of the Faro Peak formation at Faro Peak.* ***(a)*** *Micaceous siltstone; and* ***(b)*** *tabular-bedded micaceous siltstone. Brown-handled hammer (33 cm) for scale.*

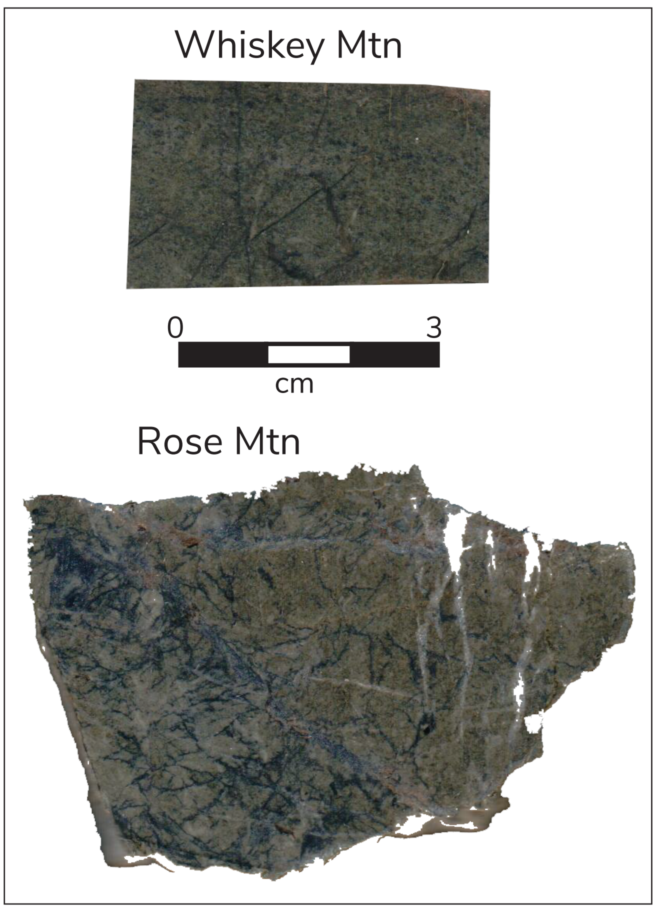

Figure 12. *Comparison between green wacke at eastern Whiskey Mountain area* ***(upper)*** *and unsheared green wacke overlying basalt at Rose Mountain area* ***(lower)****.*

siltstone, and feldspathic arenite at the Faro Peak locality. Micaceous strata are characteristic of Upper Triassic overlap assemblage units in association with Yukon-Tanana terrane, Slide Mountain terrane, and ancestral Cordilleran margin from eastern Alaska to northern British Columbia (Beranek and Mortensen, 2011).

Lower member basalt from Rose Mountain is lithologically distinct from that of the Permian Campbell Range formation to the northeast of the Vangorda fault and its apparent conformable nature above Carnian to Rhaetian limestone units indicates a Late Triassic depositional age. The lack of epidote streaking and green chlorite-alteration also suggests it is distinct from basalt mapped as basal Faro Peak formation by Pigage (2004) and Jennings *et al.* (1978) south of Rose Mountain (Fig. 3). Pigage (2004) speculated that this ‘basal basalt’ is unrecognized Campbell Range formation as the N-MORB (normal mid-ocean ridge basalt) whole-rock geochemical compositions of this unit are indistinguishable from Permian units in the Faro area. The geochemical signatures of Campbell Range formation rocks in the Finlayson Lake area are also similar (e.g., Piercey *et al.*, 2012). Therefore, based on the mineralogical and geochemical similarities between the ‘basal basalt’ of Faro Peak formation and Campbell Range formation from the Faro and Finlayson Lake areas, the ‘basal basalt’ locality south of Rose Mountain outlined in Pigage (2004) is herein reassigned to Campbell Range formation.

An outcrop of green basalt reported by Wiest and Beranek (2019) near the Dena Cho Trail was investigated in summer 2019 to understand its relationship with the Faro Peak and Campbell Range formations (Fig. 8). This green basalt contains epidote streaking and local to pervasive chlorite-carbonate alteration suggesting an affiliation with the Permian Campbell Range formation. Its location near lower and upper member units of the Faro Peak formation suggests it may be the result of an east-northeast trending fault splay in the area (Fig. 8).

Lower member–upper member contact relationships

Repeater Hill

The contact between lower member and upper member units at Repeater Hill is well constrained (Fig. 6). Upper Triassic limestone and argillite units of the lower member crop out directly below a bed of pebble to cobble, matrix-supported, polymictic conglomerate that contains clasts of micaceous quartzite, schist, grey and black chert, green to tan volcanic rocks, and sedimentary rocks (Fig. 13a). This conglomerate marks the base of the upper member and is consistent with the map interpretations of Pigage (2004). Above this conglomerate, micaceous argillite separates these units from massive, matrix to clast-supported conglomerate that comprises the bulk of Repeater Hill and locally contains porphyry and intrusive rock clasts (Fig. 13b,c; Wiest and Beranek, 2019).

Faro Peak

At least 800 m of upper member stratigraphy is exposed above the lower member–upper member contact at Faro Peak (Fig. 14). Subvertical, tan to brown, massive to thin-bedded, medium to very coarse grained arenite units scour into, and are interbedded with, wavy laminated, micaceous siltstone to argillite (Fig. 15a–d) above the saddle ~600 m northeast of Faro Peak. This saddle separates these upper member units from tabular, lower member micaceous siltstone. The contact between the lower and upper members is drawn at the first occurrence of coarse-grained sandstone (Fig. 3) and is consistent with the map interpretations of Pigage (2004).

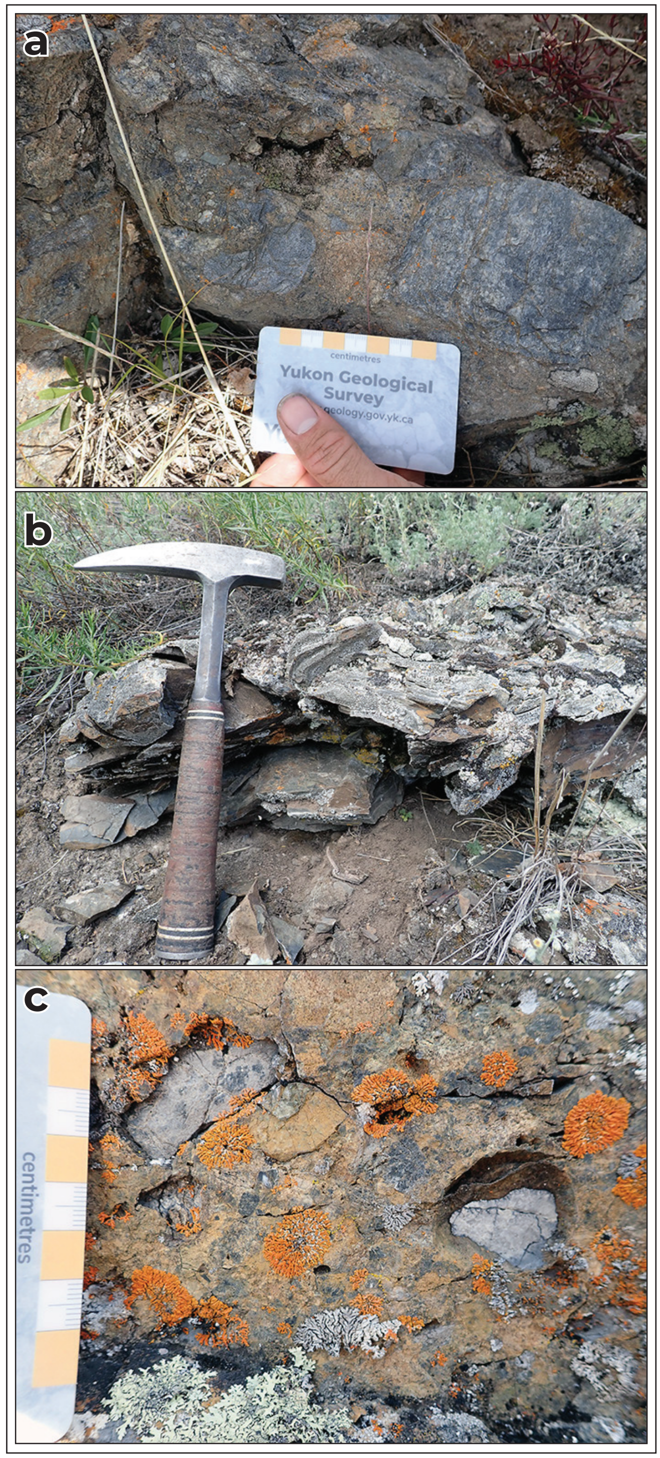

Figure 13. *Field photographs of upper member of the Faro Peak formation at Repeater Hill.* ***(a)*** *Matrix-supported conglomerate with quartzite, volcanic, and sedimentary clasts;* ***(b)*** *weakly folded micaceous argillite; and* ***(c)*** *normally graded bed in matrix-supported conglomerate. Brown-handled hammer (33 cm).*

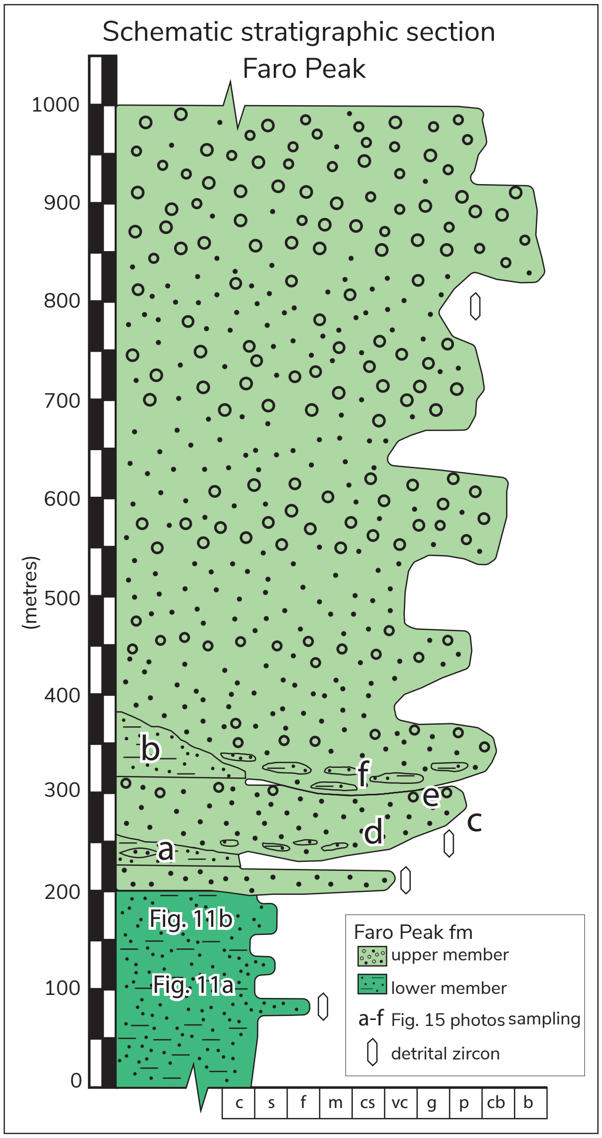

***Figure 14.** Schematic stratigraphic section of the lower and upper members of the Faro Peak formation at Faro Peak. Samples are from the 2018 and 2019 field seasons. Abbreviations same as Figure 4.*

Coarse-grained beds of feldspathic to lithic feldspathic arenite at the Faro Peak locality contain wavy laminated, micaceous argillite rip-up clasts and are locally overlain by conglomerate with clasts of grey and black chert, grey quartzite, tan volcanic rocks, and limestone (Fig. 15e). Upsection, these rip-up clasts become coarser (>10 cm) and suggest more intense scouring of argillaceous interbeds (Fig. 15f). The increase in coarse-grained sandstone, conglomerate, and rip-up clast size suggests an overall coarsening-upward sequence that continues to the summit of Faro Peak. Wiest and Beranek (2019) reported granule to cobble, matrix to clast-supported, polymictic conglomerate units containing clasts of porphyry and felsic intrusive rocks that are intercalated with very coarse grained to granule feldspathic and lithic arenite units upsection at the summit of Faro Peak and an adjacent peak ~4 km to the northwest.

Central Whiskey Mountain

The upper member of the Faro Peak formation consists of tightly folded, thin to medium-bedded, locally calcareous, micaceous feldspathic to lithic feldspathic arenite and micaceous siltstone units near the center of Whiskey Mountain, ~2.5 km northeast of Faro (Fig. 16a,b). These units occur both above and below matrix-supported conglomerate that dips gently to moderately towards the Tintina Trench and shows normally graded bedding (Fig. 16c). Conglomerate clasts include quartzite, schist, limestone, tan volcanic rocks, and pyroxenite. Below the conglomerate beds, fine-grained rocks are pervasively sheared by a fault that juxtaposes the upper member with the Snowcap assemblage (Fig. 16d). Locally, polymictic conglomerate was observed in faulted contact with these finer-grained units (Fig. 16e). It appears that fine-grained strata accommodated the majority of strain at this locality, whereas conglomerate facies are more resistant, generally appear less deformed, and contain a slight to moderate foliation (Fig. 16f) and local brittle fracturing and faulting.

Blind Creek–Dena Cho Trail

The contact between the lower and upper members is not exposed near the Blind Creek–Dena Cho Trail locality (Fig. 8). Outcrops along the southern bank of Blind Creek consist of matrix-supported conglomerate that overlies limestone and/or calcareous argillite, possibly indicating its stratigraphic position in the upper member, similar to calcareous units near central Whiskey Mountain (Fig. 17a). Upper member exposures at this locality mostly consist of matrix to clast-supported polymictic conglomerate. Clast components include green to grey quartzite, schist, black and grey chert, intermediate to mafic volcanic and intrusive rocks, and subordinate limestone, basalt, and sedimentary rocks that resemble the lower member of the Faro Peak formation (Fig. 17c,d).

Figure 15. *Field photographs of the upper member of the Faro Peak formation at Faro Peak.* ***(a)*** *Sandstone channel in interbedded micaceous argillite and siltstone;* ***(b)*** *wavy laminated argillite;* ***(c)*** *outcrop of sheet sandstone (s) and conglomerate (c) interbeds;* ***(d)*** *coarse-grained lithic feldspathic arenite (s bed from Fig. 15c);* ***(e)*** *matrix-supported conglomerate (c bed from Fig. 15c); and* ***(f)*** *disk-shaped rip-up clasts of wavy laminated argillite in very-coarse sandstone. Brown-handled hammer (33 cm) and geologist (180 cm) for scale.*

Figure 16. *Field photographs of the upper member of the Faro Peak formation at central Whiskey Mountain.* ***(a)*** *Recumbent fold in fine-grained, micaceous sandstone and siltstone;* ***(b)*** *calcareous sandstone;* ***(c)*** *Normally graded bedding in coarse-grained sandstone and matrix-supported conglomerate;* ***(d)*** *uniformly sheared fine-grained, micaceous sandstone and siltstone;* ***(e)*** *west-dipping fault separating conglomerate and fine-grained units; and* ***(f)*** *well foliated, clast-supported conglomerate. Brown-handled hammer (33 cm) for scale.*

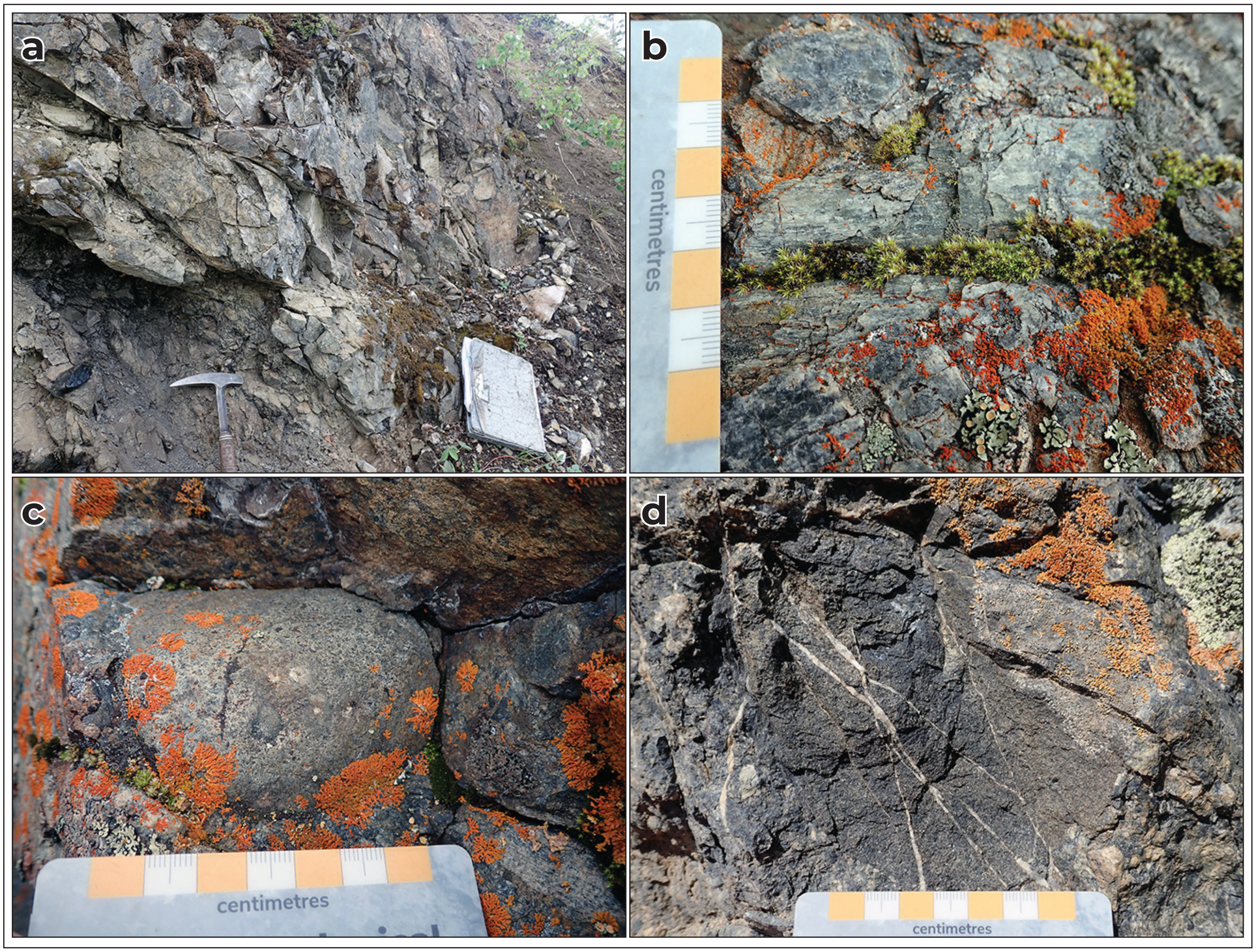

***Figure 17.** Field photographs of the upper member of the Faro Peak formation at Blind Creek and Dena Cho Trail. **(a)** Calcareous unit overlain by normally graded, matrix-supported conglomerate; **(b)** green quartzite clast; **(c)** equigranular gabbro clast; and **(d)** dark grey sandstone clast. Brown-handled hammer (33 cm) for scale.*

Interpretation

The upper member of the Faro Peak formation overlies Upper Triassic limestone units that correlate with the base of the Rose Mountain section, micaceous siltstone and feldspathic arenite units that are potentially the upper part of the lower member, and Snowcap assemblage metasedimentary and eclogitic rocks that crop out below the lower member. These observations suggest that the basal contact of the upper member is an unconformity, however, the interbedded micaceous argillite and conglomerate at Repeater Hill, and interbedded micaceous siltstone, argillite, and coarse-grained sandstone to conglomerate at Faro Peak, suggest a transitional contact between the lower and upper members. A potential third occurrence of a transitional contact is located at central Whiskey Mountain where locally calcareous micaceous siltstone and feldspathic arenite units of the upper member (e.g., Pigage, 2004) are interbedded with upper member conglomerate facies.

There are a few working hypotheses that explain the transitional and unconformable contact relationships between the lower and upper members: (1) micaceous units at Faro Peak and Repeater Hill are fine-grained parts of the upper member and do not belong to the lower member. This compares well with central Whiskey Mountain where micaceous siltstone and feldspathic arenite units have previously been mapped as the upper member (Pigage, 2004); (2) lower and upper member units comprise part of a syndepositional synform. Bedding is moderately to steeply dipping and the contact with lower member and upper member units appears transitional only near the trace of the Vangorda fault. Towards the Tintina Trench, lower member units are not exposed and massive, polymictic conglomerate units of the upper member sit unconformably on Snowcap assemblage; and (3) lower member units are not laterally continuous and Upper Triassic limestone and argillite beds are correlative with micaceous siltstone and feldspathic arenite units. This last hypothesis requires that micaceous sedimentary rocks in the Faro area are not laterally continuous, suggesting that different units contain a different provenance and became interfingered in the Faro Peak basin(s).

Discussion and future work

The lower member of the Faro Peak formation should be reassigned to a new formation because it is lithologically distinct and its lower and upper contacts are defined by unconformities. This new formation likely consists of a lower, limestone-argillite unit and an upper, basalt-wacke-feldspathic arenite unit. It is uncertain if micaceous units currently mapped as the lower member of the Faro Peak formation at central Whiskey Mountain, Repeater Hill, and the base of the Faro Peak section are part of this new formation, or, if they instead represent fine-grained parts of the upper member of the Faro Peak formation. It is also uncertain if basalt and wacke units at Rose Mountain correlate with the wacke and feldspathic arenite units along the eastern ridge of Whiskey Mountain. Future detrital zircon U-Pb-Hf studies will assist in identifying the stratigraphic position of these units and determine if some, or all, of the lower member of the Faro Peak formation should be assigned to a new formation.

Preliminary conclusions

Field investigations of Upper Triassic to Lower Jurassic rock units near Faro have uncovered new details about the regional stratigraphy of the southern Tay River map area. The lower member of the Faro Peak formation likely represents part of an Upper Triassic overlap assemblage that covered the Yukon-Tanana and Slide Mountain terranes and ancestral North American margin, similar to other Upper Triassic strata that crop out along the eastern edge of the Intermontane terranes from eastern Alaska to northern British Columbia (Beranek and Mortensen, 2011; Golding *et al.* 2016). Basal conglomerate units of the lower member near Rose Mountain sit unconformably on the Snowcap assemblage and indicate that Yukon-Tanana terrane basement was locally exhumed to the surface by Late Triassic time. Black and grey chert clasts furthermore indicate that lower member sand and gravel were also partially sourced from Paleozoic rock units of the adjacent Slide Mountain terrane. These observations suggest that the suture between the Yukon-Tanana and Slide Mountain terranes accommodated early Late Triassic subsidence during regional plate convergence, initiation of a new east-dipping subduction zone, and collisional processes along the outboard edge of northwestern North America (*e.g.*, Nelson *et al.*, 2013).

The lithology and stratigraphic character of upper member strata are consistent with synorogenic deposition related to Early Jurassic exhumation of the northern Intermontane terranes in central Yukon (Colpron *et al.* 2015). The upper member is massively bedded, >800 m-thick, and its basal units are dominated by pebble to cobble-sized clasts of limestone, argillite, and volcanic rocks, whereas the exposed top also contains up to boulder-sized clasts of mafic to felsic intrusive rocks. These observations are consistent with progressive unroofing and suggest proximity to a basin-bounding structure, such as the proto-Vangorda fault (cf. Tempelman-Kluit, 1972). Faro Peak basin subsidence and exhumation of the Snowcap assemblage was likely controlled by major extensional to transcurrent structures (*e.g.*, Colpron *et al.*, 2015) similar to the Willow Lake fault in central Yukon (Knight *et al.*, 2013) that accommodated the Early Jurassic exhumation of Yukon-Tanana basement. Clasts in upper member conglomerate (Wiest and Beranek, 2019) also suggest that basin-filling along the Yukon-Tanana and Slide Mountain suture that initiated during the early Late Triassic persisted until or became active again during the Early Jurassic. Lower and upper member strata of the Faro Peak formation are cut by the Vangorda fault (see Fig. 8) and confirm that this terrane-bounding fault underwent post-Early Jurassic motion. The Jules Creek fault in the Finlayson Lake area is the southern equivalent to the Vangorda fault and is similarly suggested to have accommodated subsidence and strike-slip motion that occurred until early Mesozoic time (Murphy *et al.*, 2006). Future studies of the Faro Peak formation will further assess the potential correlations between clastic units in the Finlayson Lake and southern Tay River map areas. These results combined with continued investigations into the stratigraphic relationships between lower and upper member units will provide new insights into the evolution of the Yukon-Tanana–Slide Mountain terrane boundary and further constrain plate tectonic models for the early growth of the Canadian Cordillera.

Acknowledgements

This is a product of the Geo-mapping for Energy and Minerals (GEM) program at Natural Resources Canada. A special thanks to the Yukon Geological Survey for field logistics and helicopter support to the Rose Mountain area. Thank you to reviewer Don Murphy for thoughtful and constructive comments that significantly improved this manuscript.

References

Beranek, L.P. and Mortensen, J.K., 2011. The timing and provenance record of the Late Permian Klondike orogeny in northwestern Canada and arc-continent collision along western North America. Tectonics, vol. 30, TC5017.

Clark, A.D., 2017. Tectonometamorphic history of mid-crustal rocks at Aishihik Lake, southwest Yukon. Unpublished MSc thesis, Simon Fraser University, British Columbia, Canada, 153 p.

Colpron, M., Crowley, J.L., Gehrels, G.E., Long, D.G.F., Murphy, D.C., Beranek, L.P. and Bickerton, L., 2015. Birth of the northern Cordilleran orogen, as recorded by detrital zircons in Jurassic synorogenic strata and regional exhumation in Yukon. Lithosphere, vol. 7, p. 541–562.

Colpron, M., Nelson, J.L. and Murphy, D.C., 2006. A tectonostratigraphic framework for the pericratonic terranes of the northern Canadian Cordillera. In: Paleozoic Evolution and Metallogeny of Pericratonic Terranes at the Ancient Pacific Margin of North America, Canadian and Alaskan Cordillera, M. Colpron and J.L. Nelson (eds.), Geological Association of Canada Special Paper 45, p. 1–23.

Dusel-Bacon, C., Lanphere, M.A., Sharp, W.D., Layer, P.W. and Hansen, V.L., 2002. Mesozoic thermal history and timing of structural events for the Yukon-Tanana Upland, east-central Alaska: $^{40}Ar/^{39}Ar$ data from metamorphic and plutonic rocks. Canadian Journal of Earth Sciences, vol. 39, p. 1013–1051.

Gabrielse, H., Murphy, D.C. and Mortensen, J.K., 2006. Cretaceous and Cenozoic dextral orogen-parallel displacements, magmatism, and paleogeography, north-central Canadian Cordillera. In: Paleogeography of the North American Cordillera: Evidence For and Against Large-Scale Displacements, Haggard, J.W., Enkin, R.J. and Monger, J.W.H. (eds.), Geological Association of Canada, Special Paper 46, p. 255–276.

Golding, M.L., Mortensen, J.K., Ferri, F., Zonneveld, J.-P. and Orchard, M.J., 2016. Determining the provenance of Triassic sedimentary rocks in northeastern British Columbia and western Alberta using detrital zircon geochronology, with implications for regional tectonics. Canadian Journal of Earth Sciences, vol. 53, p. 140–155.

Jennings, D.S., Jilson, G.A., Hanson, D.J. and Franzen, J.P., 1978. Geology Anvil District map area, Unpublished Cyprus Anvil Mining Corporation internal company report 1:50 000 scale.

Johnston, S.T., Mortensen, J.K. and Erdmer, P., 1996. Igneous and metaigneous age constraints for the Aishihik metamorphic suite, southwest Yukon. Canadian Journal of Earth Sciences, vol. 33, p. 1543–1555.

Knight, E., Schneider, D.A. and Ryan, J.J., 2013. Thermochronology of the Yukon-Tanana terrane, west-central Yukon: Evidence for Jurassic extension and exhumation in the northern Canadian Cordillera. Journal of Geology, vol. 121, p. 371–400.

Mihalynuk, M.G., Nelson, J.A. and Diakow, L.J., 1994. Cache Creek terrane entrapment: Oroclinal paradox within the Canadian Cordillera. Tectonics, vol. 13, p. 575–595.

Murphy, D.C., Mortensen, J.K., Piercey, S.J., Orchard, M.J. and Gehrels, G.E., 2006. Mid-Paleozoic to early Mesozoic tectonostratigraphic evolution of the Yukon-Tanana and Slide Mountain terranes and affiliated overlap assemblages, Finlayson Lake massive sulphide district, southeastern Yukon. In: Paleozoic Evolution and Metallogeny of Pericratonic Terranes at the Ancient Pacific Margin of North America, Canadian and Alaskan Cordillera, M. Colpron and J.L. Nelson (eds.), Geological Association of Canada Special Paper 45, p. 75–105.

Nelson, J.L., Colpron, M. and Israel, S. 2013. The Cordillera of British Columbia, Yukon, and Alaska: Tectonics and Metallogeny. In: Tectonics, Metallogeny and Discovery: The North American Cordillera and Similar Accretionary Settings, M. Colpron, T. Bissig, B.G. Rusk and J.F.H. Thompson (eds.), Society of Economic Geologists, Special Publication 17, p. 53–109.

Orchard, M.J., 2006. Late Paleozoic and Triassic conodont faunas of Yukon and northern British Columbia and implications for the evolution of the Yukon-Tanana terrane. In: Paleozoic Evolution and Metallogeny of Pericratonic Terranes at the Ancient Pacific Margin of North America, Canadian and Alaskan Cordillera, M. Colpron and J.L. Nelson (eds.), Geological Association of Canada Special Paper 45, p. 229–260.

Piercey, S.J., Murphy, D.C. and Creaser, R.A., 2012. Lithosphere-asthenosphere mixing in a transform-dominated late Paleozoic backarc basin: Implications for northern Cordilleran crustal growth and assembly. Geosphere, vol. 8, no. 3, p. 716–739.

Pigage, L.C., 2004. Bedrock geology compilation of the Anvil District (parts of NTS 105K/2, 3, 5, 6, 7, and 11), central Yukon. Yukon Geological Survey, Bulletin 15, 103 p.

Porter, C., Morin, P., Howat, I., Noh, M-J., Bates, B., Peterman, K., Keesey, S., Schlenk, M., Gardiner, J., Tomko, K., Willis, M., Kelleher, C., Cloutier, M., Husby, E., Foga, S., Nakamura, H., Platson, M., Wethington, M. Jr., Williamson, C., Bauer, G., Enos, J., Arnold, G., Kramer, W., Becker, P., Doshi, A., D'Souza, C., Cummens, P., Laurier, F. and Bojesen, M., 2018. ArcticDEM, https://doi.org/10.7910/DVN/OHHUKH, Harvard Dataverse, vol. 1 [accessed November, 2019].

Staples, R.D., Gibson, H.D., Colpron, M. and Ryan, J.J., 2016. An orogenic wedge model for diachronous deformation, metamorphism, and exhumation in the hinterland of the northern Canadian Cordillera. Lithosphere, vol. 8, no. 2, p. 165–184.

Tempelman-Kluit, D.J., 1972. Geology and origin of the Faro, Vangorda, and Swim concordant zinc-lead deposits, central Yukon Territory. Geological Survey of Canada, Bulletin 208, 73 p.

Tempelman-Kluit, D.J., 1979. Five occurrences of transported synorogenic clastic rocks in Yukon Territory. Geological Survey of Canada, Paper 79-1A, p. 1–12.

Topham, M.J., Allan, M.M., Mortensen, J.K., Hart, C.J.R., Colpron, M. and Sack, P.J., 2016. Crustal depth of emplacement of the Early Jurassic Aishihik and Tatchun batholiths, west-central Yukon. *In:* Yukon Exploration and Geology 2015, K.E. MacFarlane (ed.), Yukon Geological Survey, p. 233–251.

University of Minnesota, 2018. Polar Geospatial Center, https://www.pgc.umn.edu [accessed November, 2019].

Wiest, A.C., Beranek, L.P., 2019. Stratigraphy of the Faro Peak formation, central Yukon: New field observations of Jurassic synorogenic sedimentation along the Yukon-Tanana–Slide Mountain terrane boundary. In: Yukon Exploration and Geology 2019, K.E. MacFarlane (ed.), Yukon Geological Survey, p. 127–142.

Yukon Geological Survey, 2019. Yukon Digital Bedrock Geology. Yukon Geological Survey, http://data.geology.gov.yk.ca/Compilation/3, [accessed November, 2019].